Journal of Nuclear Materials 386–388 (2009) 466–470

Contents lists available at ScienceDirect

Journal of Nuclear Materials

journal homepage: www.elsevier.com/locate/jnucmat

Strengthening of the RAFMS RUSFER-EK181 through nanostructuring surface layers

A.V. Panin [a,*], V.M. Chernov [b], M.V. Leontieva-Smirnova [b], E.A. Melnikova [a]

[a] Institute of Strength Physics and Materials Science, SB RAS, 634021 Tomsk, Russia
[b] A.A. Bochvar Research Institute of Inorganic Materials, 123060 Moscow, Russia

A B S T R A C T

The special features of plastic deformation as well as mechanical properties of strengthened RAFMS RUSFER – EK181 high-alloy steel were studied. Surface nanostructuring through ultrasonic impact treatment increases strength properties of the reduced activated ferritic–martensitic steel RUSFER – EK181. A nanostructure within the surface layers of the specimens was formed. Using scanning tunnelling microscope reveals a new mechanism of mesoscale-level plastic deformation of nanostructured surface layers as doubled spirals of extruded material mesobands. A linear dependence of their sizes on strain as well as thickness of strengthened layer was obtained.

© 2009 Elsevier B.V. All rights reserved.

1. Introduction

Surface nanostructuring of structural materials has attracted significant scientific interest because of considerable increase of their strength characteristics, on the one hand, and their simplicity and low cost, on the other hand. Conventionally, a nanostructured surface layer can be formed in a bulk material by means of various methods, namely Esonix ultrasonic impact treatment (EUIT) [1], ultrasonic shot peeping (USSP) [2–4], surface mechanical attrition treatment (SMAT) [5], electron beams [6,7], ball-milling [8], etc. Such treatment of the surface layers changes the dislocation structure in the material, reduces grains and subgrains to the nano- and submicron scale, widens the misorientation angles and so on. Thus, it gives the possibility to control the deformation behavior as well as to influence on the mechanical properties of metals and alloys. Surface nanostructuring would be expected to improve the overall properties, yield and tensile strength [5,6], fatigue life [9], wear and corrosion resistance [10] and performance of materials.

One of the ways to increase thermal stability of nanostructured surface layers is to combine thermal and mechanical treatments of structural steels. In Ref. [11], we suggested to perform the ultrasonic impact treatment between quenching and ageing of reduced activated ferritic–martensitic steel (RAFMS) RUSFER – EK181. Firstly, it significantly reduces internal stresses, which appear under ultrasonic impact treatment. Secondly, precipitation of vanadium carbide particles at the grain boundaries during ageing of the specimens with nano-(submicro-) crystalline surface layers should considerably increase its thermal stability. In the present research, the effect of nanocrystalline structure within the surface layers of ferritic–martensitic steel RUSFER – EK181 on the character of plastic deformation and mechanical properties is studied.

2. Materials and experimental procedure

Specimens of ferritic–martensitic steel RUSFER – EK181 (steel content is shown in Table 1), which were preliminary quenched (at 1080 °C during 1 h) and then subjected to ultrasonic impact treatment followed by ageing (at 720 °C during 3 h), were used as a material for investigation.

The ultrasonic impact treatment of one or both sides of the plate was performed using IL-4 unit by excitation of ultrasonic vibrations in the treatment tool. The treatment tool was a hard alloy rod 5 mm in diameter with a rounded end. The vibration amplitude and frequency of the waveguide working surface made up 15 μm and 24 kHz, respectively. The deforming tool was pressed to the surface of the treated plate with a static load of 200 N. The plate thickness comprised 2.0 and 0.6 mm, the depth of the modified surface layer was 100, 200 and 300 μm. Thus, the fraction of the structurally modified layer in the volume of the specimen varied from 5% to 50%. The depth of the strengthened surface layer was evaluated by measuring the microhardness $H\mu$ along the cross-section of the specimens by means of a PMT-3 microhardness meter using Vickers pyramid. Indentation load made up 50 g.

Specimens for mechanical testing in the form of dumbbell with gage part measured 3 × 1 × 30 mm were cut out by wire electrical discharge machine. In order to discuss the effect of ultrasonic treatment on the strain-induced relief, the specimen surfaces before and after hardening were treated in proper way. All the specimens were polished using 1 μm diamond paste and finely cleaned in acetone followed by air drying. Tension and compression testing was carried out with 0.2 mm/min loading rate using an INSTRON

* Corresponding author. Tel.: +7 3822 286 979; fax: +7 3822 492 576.
E-mail address: pav@ispms.tsc.ru (A.V. Panin).

0022-3115/$ - see front matter © 2009 Elsevier B.V. All rights reserved.
doi:10.1016/j.jnucmat.2008.12.162

Table 1
Chemical composition of the RAFMS RUSFER – EK181.

C	Si	Mn	Cr	Ni	Mo	W	V	Nb	Ta	B	N	Ti	Zr	Cu	Co
0.1–0.2	0.3–0.5	0.50.8	10–12	0.1	0.01	1.2	0.2–1	0.01	0.05–0.2	0.003–0.006	0.02–0.15	0.03–0.3	0.05–0.2	0.1	0.01

testing machine. The evolution of strain-induced surface relief of the loaded specimens was studied with the help of a scanning tunnelling microscope (STM) Nanometer – 1. Defect substructure and phase composition of the investigated specimens were determined by transmission electron microscopy (EM-125K) at accelerating voltage 125 kV.

3. Experimental data

Fig. 1 shows the microstructure and selected area electron diffraction (SAED) pattern of ferritic–martensitic steel RUSFER – EK181 subjected to quenching, ultrasonic impact treatment and ageing. There is less evidence for a martensite structure, the equiaxed grains and subgrains with average grain size ~100 nm are found in the strengthened surface layer. The scalar dislocation density exceeds 6.5×10^{10} cm^{-2}. The SAED pattern obtained using the same size of selection aperture shows that after surface strengthening the diffraction spots have become diffuse indicating an increase in misorientation between neighboring grains (Fig. 1(c)). Moreover, no evidence of $M_{23}C_6$ carbide particles are observed, the particles of vanadium carbide V_2C consist the main carbide phase (Fig. 1(b)).

The formation of the nano-(submicro-) crystalline structure within the surface layer of the RAFMS RUSFER – EK181 specimen causes the localized character of plastic deformation under uniaxial tension test. Arrangement of a great number of STM-images that allows large-area surface investigation with ultra-high resolution has shown intertwined mesobands of extruded material forming the conjugate directions of maximum tangential stresses over the entire gage part of a loaded specimen (Fig. 2). Within the mesobands a non-crystallographic displacement of lamellae relative to each other takes place. Besides, each lamella consists in a many fine folds (Fig. 2(d)). Fig. 3 depicts the linear dependence of the width of the mesobands of extruded material on the strain. Meso-

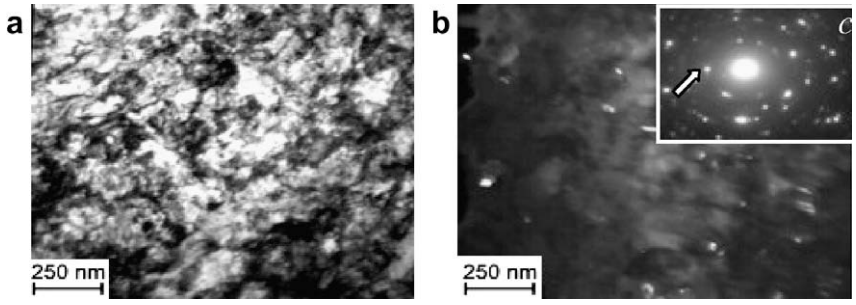

Fig. 1. Bright-field TEM image (a), dark-field TEM image in the V_2C [0 1 1] reflection (b), and selected area electron diffraction pattern (inset in (b)) of the surface layer of RAFMS RUSFER – EK181 specimen subjected to quenching, ultrasonic impact treatment and ageing; (the arrow indicates the reflection in which the dark-field image was taken).

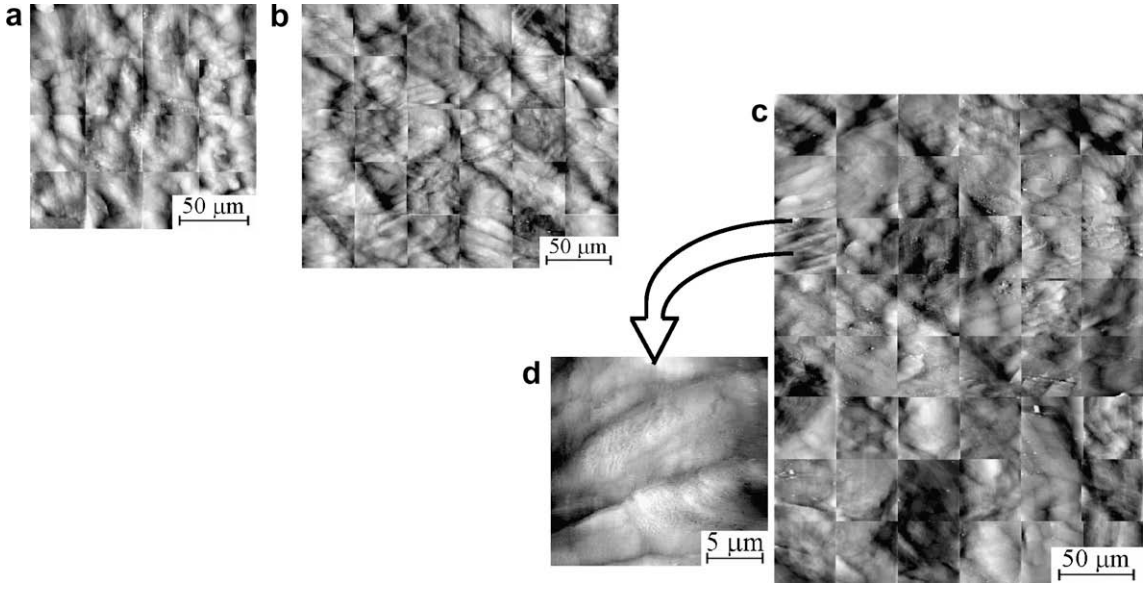

Fig. 2. STM-images of the surface layer of a RAFMS RUSFER – EK181 specimen subjected to quenching, ultrasonic impact treatment followed by ageing; tension: $\varepsilon = 4\%$ (a), 6% (b) and 10% (c, d). Thickness of the specimens is 2 mm. Surface height is represented by grey level, over a range from darkest (minimum height) to lightest (maximum height).

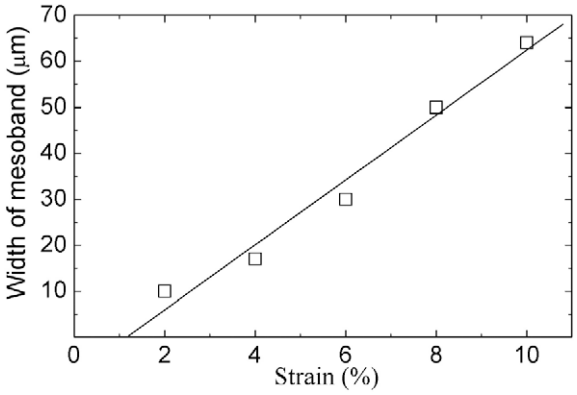

Fig. 3. The width of mesobands of localized deformation vs. strain.

band width gradually rises with strain and reaches 65 μm at $\varepsilon = 10\%$.

The change of ultrasonic treatment power allows varying the depth and microhardness of the hardened layer in a wide range. In the present study, three different modes of ultrasonic impact treatment were used (Fig. 4). The first mode of treatment results in slight strengthening of the RAFMS RUSFER – EK181 specimen: the depth of the hardened surface layer, defined as a depth from the surface at which the hardness drops to nearly bulk value, does not exceed $d = 100$ μm, and the maximum value of microhardness is equal to 3800 MPa. Eventually, with increasing the power of ultrasonic energy, the depth of the modified surface layer increases to 300 μm and the microhardness grows up to 4200 MPa.

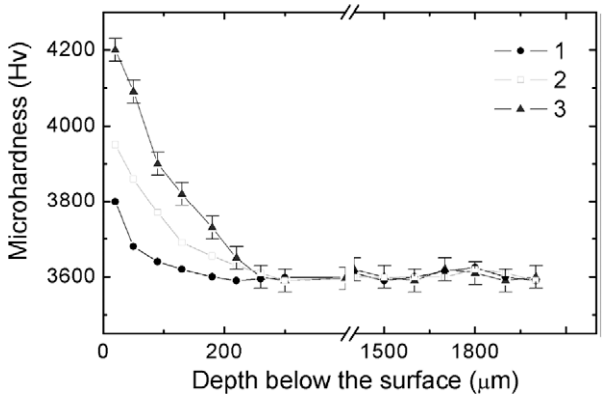

Fig. 4. Microhardness of the RAFMS RUSFER – EK181 specimens subjected to quenching, ultrasonic impact treatment and ageing as a function of the depth below the surface; depth of the hardened layer is 100 (1), 200 (2) and 300 μm (3).

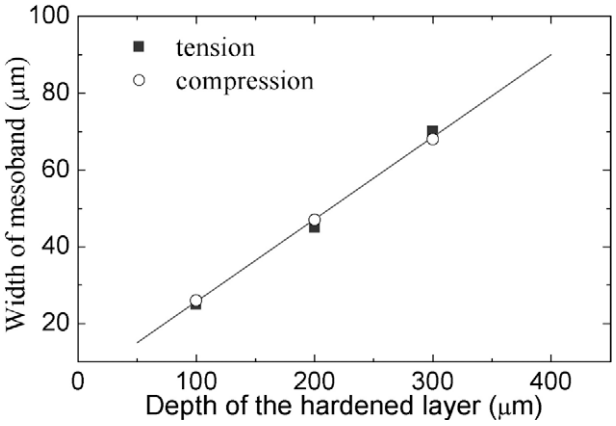

Fig. 6. The width of mesobands of localized deformation vs. depth of the hardened surface layer.

It was found out that the dimensions of the mesobands of extruded material do not depend on the type of loading and the thickness of the specimens, and are determined by the depth of the nano-(submicro-) crystalline surface layer. As shown in Fig. 5(a), under compression of the specimens with the depth of the hardened layer of 100 μm, the width of the mesobands does not exceed 25 μm. If the depth of the modified layer increases up to 200 μm, the dimensions of the mesobands grow to ~30–40 μm (Fig. 5(b)). Ultimately, at the hardened layer depth of 300 μm, the mesoband width reaches 60 μm (Fig. 5(c)). Similar linear dependence of the width of the intertwined mesobands of extruded material on the depth of the hardened surface layer was found in the RAFMS RUSFER – EK181 specimens subjected to uniaxial tension tests (Fig. 6).

Uniaxial tension tests have shown that the thickness of the hardened surface layer significantly influences on the mechanical characteristics of RAFMS RUSFER – EK181 specimens. The formation of the thin hardened layer (100 μm) significantly increases yield point of the test specimens (Fig. 7, curve 2). Indeed, the maximum ultimate stress is observed after ultrasonic impact treatment of both sides of the specimens (Fig. 7, curve 3). It should be emphasized that the increase of strength properties of loaded specimens is accompanied by the decrease of their ductility.

The maximum strength properties are obtained at an optimal ratio of the hardened layer depth and specimen thickness. For example, if we reduce specimen thickness from 2 to 0.8 mm while keep constant the depth of the hardened surface layer (300 μm), the yield stress reaches the highest value. At the same time, strong localization of plastic flow in the specimen, in which the nano-(submicro-) crystalline layer volume comprises 40% of its

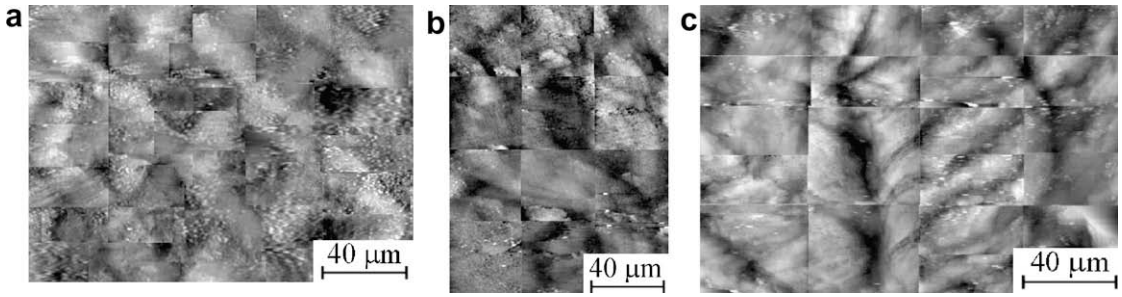

Fig. 5. STM-images of mesobands of localized deformation on the surface of the loaded RAFMS RUSFER – EK181 specimens with the depth of the hardened layer of 100 (a), 200 (b) и 300 μm (c); tension: $\varepsilon = 2\%$. Thickness of the specimens is 0.6 mm. Surface height is represented by grey level, over a range from darkest (minimum height) to lightest (maximum height).

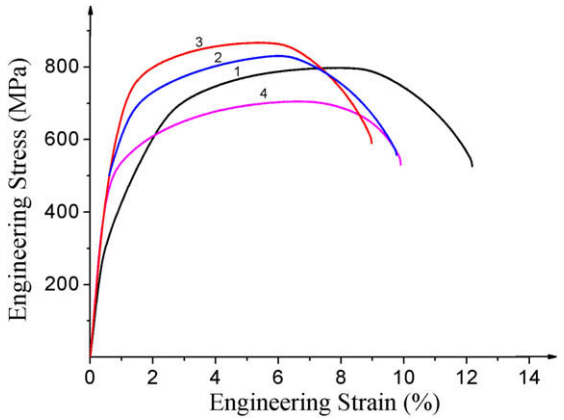

Fig. 7. Tensile engineering stress–strain curves for the RAFMS RUSFER – EK181: untreated (1), subjected to intermediate ultrasonic treatment at one (2, 4) and both sides of the specimen (3). $T = 300$ K. Depth of the hardened layer is 100 (2) and 300 μm (3, 4). Thickness of the specimens is 2 mm (1–3) and 0.8 mm (4).

thickness, results in simultaneous reduction of strength and ductility of the material (Fig. 7, curve 4).

4. Discussion

According to the Hall–Petch relationship, the yield strength of the nanostructured surface layer significantly exceeds the yield strength of the unmodified bulk material. Therefore, at the beginning of loading the nanostructured surface layer experiences elastic deformation, while the coarse-grain bulk material is already involved in plastic deformation. If the nanostructured surface layer/bulk material system is subjected to uniaxial compression, the nanostructured surface layer will wrinkle due to the competition between the effects of its elastic bending, which favors long wavelength buckles, and plastic deformation of the bulk material, which favors short wavelength ones. The competition between the bending-dominated deformation of the nanostructured surface layer and the shear-dominated deformation of the bulk material causes wrinkling of the nanostructured surface layer in response to the relaxation of the applied strain. The similar mechanism of wrinkling in thin metal films on polymer substrates under thermal and mechanical loading is clearly identified and explained in [12]. Wrinkling of the nanostructured surface layer/bulk material system also occurs in the case of uniaxial tensile deformation, because the system undergoes compressive strains perpendicular to the direction of the load due to reconstruction of inter-atomic bonds.

The periodic corrugation of the nanostructured surface layer follows the requirements of compatibility of retaining deformation and equilibrium at the interface between the layer and the bulk material. Such deformation-induced surface corrugation results

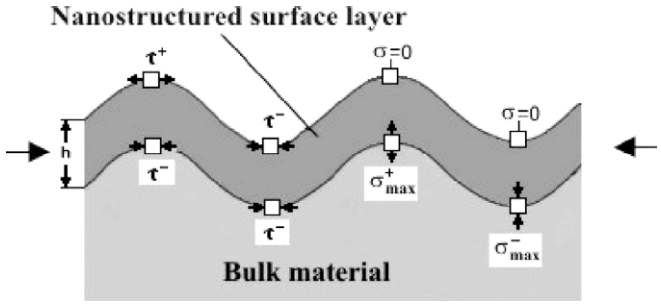

Fig. 8. Schematic diagram illustrating the state of stresses in a wrinkled nanostructured surface layer.

in a periodic distribution of normal and tangential stresses in the 'nanostructured surface layer/bulk material' system (Fig. 8). In two-dimensional case, the periodic distribution of zones subjected to normal and tangential tensile and compressive stresses has a chessboard-like pattern [13].

As Fig. 8 shows the normal stresses vary from a maximum tensile value to zero in the ridge region and from a maximum compressive value to zero in the valley region [12]. Usually, tangential stresses in the specimen under compression have only compressive value. However, if the curvature of the nanostructured layer reaches a high value, compressive tangential stresses at the top of the ridge can turn into tensile ones. The difference between deformations of the surface layer and the bulk material enhances with strain and causes increasing of amplitude and wavelength of wrinkling.

According to the principles of physical mesomechanics [14], plastic flow of a solid under any external forces is due to a local loss of its shear stability and develops as a local structural phase transformation of the crystal in zones of the plastic shear. When loading the 'nanostructured surface layer/bulk material' system, flows of local mass transfer propagate in the conjugate directions of maximum tangential stresses τ_{max} only along the zones of the chessboard-like interface with tensile normal stresses. The atomic redistribution is impossible in the local areas subjected to normal compressive stresses [15].

Under loading of the RAFMS RUSFER – EK181 specimens any shears within nanostructured surface layers propagate in the conjugate directions of maximum tangential stresses along the zones of normal tensile stresses periodically distributed at the 'nanostructured surface layer/bulk material' interface. Increasing under loading of normal tensile stresses causes rising the sizes of deformation mesobands observed with a scanning tunnelling microscope.

Any plastic shear arises in the stress concentrator zone and propagates as a relaxation process [15]. The localized shear in the direction of τ_{max} along the zones of the chessboard-like interface with normal tensile stresses generates a bending moment on the predetermined axis of the specimen in the horizontal plane. Therefore, a new stress concentrator generated in the head of the shear band relaxes by a secondary shear in the conjugate direction of τ_{max} and causes the zigzag propagation of localized deformation mesobands in the nanostructured surface layer of the RAFMS RUSFER – EK181. The extrusion of surface layer material under mesoband propagation, in turn, determines the bending moment on the predetermined axis of the specimen in the vertical plane. Intertwining mesobands of extruded material keep constant the specimen axis. Further investigations are necessary to gain insight into the nature of lamellae displacement within the mesobands.

The wavelength of normal stress oscillation and, therefore, the dimensions of the chessboard-like interface zones linearly depend on the thickness of the nanostructured layer [11]. The size of mesobands of extruded material linearly increases with the depth of the hardened surface layer formed by ultrasonic impact treatment. Since the depth of extruded material does not exceed a few micrometers, the influence of their propagation on the mechanical properties of the RAFMS RUSFER – EK181 under uniaxial tension and compression has not been revealed.

Nevertheless, strengthening of the surface layer by means of ultrasonic impact treatment has a significant effect on the mechanical properties of the RAFMS RUSFER – EK181. Formation of the nanostructured layer causes suppression of the dislocation generation in the surface layer, that most clearly evidenced by increasing yield point. At the same time, the tendency for plastic instability such as the formation of shear bands or necking is due to the decrease of ductility. As mentioned above, the hardening percentage

of the specimen is the increase in the yield point and the decrease in ductility of the RAFMS RUSFER – EK181. The enhancement of the yield strength is governed by the ratio between the thickness of the hardened layer and the total specimen thickness. Eventually, with decreasing grain size within the surface layer as well as bulk material, high propensity of nano- and ultrafine-grain materials to localization of deformation at various scale levels would cause a decrease in their strength.

5. Conclusion

The effect of ultrasonic impact treatment on the microstructure, plastic deformation and mechanical properties of the RAFMS RUSFER – EK181 has been investigated. It is shown that the formation of the nano-(submicro-) crystalline surface layer significantly increases all strength characteristics of the specimens. Increasing strength properties of RAFMS RUSFER – EK181 depends on the layer/specimen thickness ratio.

The new mechanism of mesoscale-level deformation of surface layers of reduced activated steel EK181 was revealed. It is argued that the existence of tensile and compressive normal stresses spatially varying at the interface between the nanostructured surface layer and the bulk material underlies this mechanism. Such chessboard-like distribution of stresses causes propagation of intertwined mesobands of extruded material along the conjugate directions of maximum tangential stresses. The width of extruded mesobands linearly increases with the depth of the hardened surface layer and does not depend on loading conditions (tension, compression) and specimen thickness.

Acknowledgements

The work has been financially supported by SB RAS (Project 3.6.1.1.), RFBR Grant Nos. 05-01-00767 and 07-01-13522 ofi_ts, and RF President Grant No. MD-2413. 2008.8.

References

[1] E.S. Statnikov, Guide for Application of Ultrasonic Impact Treatment for Improving Fatigue Life of Welded Structures, IIW, Doc. XIII-1757–99, International Institute of Welding, 1999.
[2] N.R. Tao, M.L. Sui, J. Lu, Nanostruct. Mater. 11 (4) (1999) 433.
[3] G. Lu, J. Lu, K. Lu, Mater. Sci. Eng. A 286 (2000) 91.
[4] X. Wu, N. Tao, Y. Hong, Acta Mater. 50 (2002) 2075.
[5] K.Y. Zhu, A. Vassel, F. Brisset, Acta Mater. 52 (2004) 4101.
[6] D.I. Proskurovsky, V.P. Rotshtein, G.E. Ozur, J. Vac. Sci. Technol. A 16 (4) (1998) 2480.
[7] R. Zenker, Adv. Eng. Mater. 6 (7) (2004) 581.
[8] C.C. Koch, Nanostruct. Mater. 2 (1993) 109.
[9] K. Lu, J. Lu, Mater. Sci. Eng. A 375–377 (2004) 38.
[10] T. Roland, D. Retraint, K. Lu, Scripta Mater. 54 (2006) 1949.
[11] A.V. Panin, V.E. Panin, Y.I. Pochivalov, in: Proceedings of International Conference MESOMECH'2006, ISPMS SB RAS, Tomsk, Russia, p. 204.
[12] V.K. Tolpygo, D.R. Clarke, Acta Mater. 46 (14) (1998) 5167.
[13] V.E. Panin, A.V. Panin, D.D. Moiseenko, Phys. Mesomech. 10 (1) (2007) 5.
[14] V.E. Panin, V.E. Egorushkin, P.V. Makarov, Physical Mesomechanics of Heterogeneous Media and Computer-Aided Design of Materials, Ed. Panin, Cambridge, 1998.
[15] V.E. Panin, V.E. Egorushkin, Phys. Mesomech. 11 (3) (2008) 105.